INTERNATIONAL JOURNAL FOR NUMERICAL METHODS IN FLUIDS, VOL. 5, 785–803 (1985).

VARIABLE PENALTY METHOD FOR FINITE ELEMENT ANALYSIS OF INCOMPRESSIBLE FLOW

HAROON S. KHESHGI* AND L. E. SCRIVEN

Department of Chemical Engineering and Materials Science, University of Minnesota, Minneapolis, MN 55455, U.S.A.

SUMMARY

A new scheme is applied for increasing the accuracy of the penalty finite element method for incompressible flow by systematically varying from element to element the sign and magnitude of the penalty parameter λ, which enters through $\nabla\cdot\mathbf{v} + p/\lambda = 0$, an approximation to the incompressibility constraint. Not only is the error in this approximation reduced beyond that achievable with a constant λ, but also digital truncation error is lowered when it is aggravated by large variations in element size, a critical problem when the discretization must resolve thin boundary layers. The magnitude of the penalty parameter can be chosen smaller than when λ is constant, which also reduces digital truncation error; hence a shorter word-length computer is more likely to succeed. Error estimates of the method are reviewed. Boundary conditions which circumvent the hazards of aphysical pressure modes are catalogued for the finite element basis set chosen here. In order to compare performance, the variable penalty method is pitted against the conventional penalty method with constant λ in several Stokes flow case studies.

KEY WORDS Variable Penalty Method Penalty Finite Element Analysis Rotating Flow

1. INTRODUCTION

For incompressible flow the mass conservation equation degenerates to the condition that the velocity field be solenoidal, i.e. divergence-free. To analyse incompressible flow, the momentum conservation equation—the Navier–Stokes equation in the case of a Newtonian fluid we consider here—must be solved subject to the solenoidal constraint.

The momentum and continuity equations can be solved simultaneously for the unknown velocity vector field and pressure field. Pressure basis functions weight the continuity equation; velocity basis functions weight the momentum equation. Coefficients of pressure basis functions serve as Lagrange multipliers that enforce the solenoidal constraint.[1] In order to get an accurate finite element solution, it has been found that *different* basis sets must be used for pressure and velocity.[1,2] We shall henceforth refer to this as the *direct mixed interpolation method.*

The ability to decouple the unknown pressure coefficients from the weighted residuals of the momentum equation became feasible with the discovery of how to adapt the penalty function idea to incompressible flow.[3,4] The key is to allow the fluid to be ever-so-slightly compressible by making pressure proportional to the divergence of velocity in what was the continuity equation, namely

$$\nabla\cdot\mathbf{v} + p/\lambda = 0 \tag{1}$$

*Present address: Lawrence Livermore National Laboratory, Livermore, CA, U.S.A.

0271–2091/85/090785–19$01.90

Received 8 December 1983
Revised 11 February 1985

and to choose the proportionality factor λ large enough that the flow is virtually incompressible. Heretofore λ has been chosen to be a constant.[5,6] In this paper we show that there can be great benefits from choosing it to be variable.

In mathematical terms λ in (1) is the *penalty parameter*. The penalty method introduced by Courant, Friedrichs and Lewy[7] is a means of minimizing a functional with respect to a constraint, an alternative to the method of Lagrange multipliers. This is done by adding to the functional the penalty parameter multiplied by a convex functional, usually the square, of the constraint residual. Under certain boundary conditions the problem of incompressible Stokes flow can be put in extremum form, i.e. it has a functional to minimize, but under a constraint, i.e. that velocity be divergence free. In practice the Galerkin weighted residual method is applied to the finite element discretization of the equations of motion; the extremum form, if it exists, is not passed through and in fact it need not exist. Instead, in the *penalty finite element method*[1,8,9] for flow problems the continuity equation is replaced by (1) and pressure is expanded in finite element basis functions that are discontinuous at the element boundaries so that (1) weighted with the pressure basis functions on each element or subdomain gives rise to algebraic equations that can be solved as an independent set.

As in the direct mixed interpolation method, pressure basis functions are chosen to be of lower order than velocity ones, and for the same reasons.[10,11] The consequence is that the coefficients of pressure basis functions can be eliminated from the Galerkin weighted residual equations of the momentum equation, thereby reducing the number of simultaneous residual equations and in turn the computational work needed to produce the coefficients of the finite element representation of $\mathbf{v}$ and p.

If the same basis sets are used for the penalty and direct mixed interpolation methods a 'penalty solution' can in principle be made as close as desired to a 'mixed interpolation solution' of the same problem by choosing the penalty parameter large enough that $\nabla\cdot\mathbf{v}=0$ is approximated well enough, i.e. that *compressibility error* is sufficiently small. This has been proved mathematically[12,13] and tested numerically.[6,14,15] *Digital truncation error* confounds principle, however. As a matrix problem the pressure-freed equations of momentum residual are ill-conditioned: the condition number of the matrix increases in direct proportion to λ and inversely as the square of the smallest element diameter, the diameter of an element being the diameter of the largest circle that can be inscribed in it.[14,16,17] In reality to avoid excessive digital truncation error, λ cannot be made too large. Whether a safe passage exists between the Scylla of compressibility error and the Charybdis of digital truncation error depends on the number of digits of accuracy of the available computer, on the size of the smallest elements into which the problem domain is tessellated, and on the ranges of interest of the parameters in the problem.[18,19] Commonly the penalty method requires a computer of high accuracy.

In this paper we show that the range of penalty parameters that produce acceptable compressibility and digital truncation errors can usually be expanded by varying the sign and magnitude of the penalty parameter λ from element to element in a certain way. The development is in terms of steady two-dimensional Stokes flow with fixed boundaries, i.e. flow lacking non-linearities, whether from inertial effects or free boundaries, although penalty methods have been applied to both.[15,20] Error estimates found by formal mathematical analysis have been extended to flow with convective inertial force, i.e. flow with non-linearities, in a related paper.[21]

The finite element formulation of the equation system for Stokes flow is described in Section 2. The rationale behind our systematic variation of λ is described in Section 3.1. As in the case of the mixed interpolation and penalty function finite element methods, our variable penalty method is subject to parasitic 'pressure modes' which are numerical artefacts to be avoided:[10,11] boundary conditions which do or do not admit pressure modes are catalogued in Section 3.2. That the

variable penalty method can give substantially greater accuracy than the conventional penalty method is demonstrated in Section 4 with examples of planar Poiseuille flow, lid-driven cavity flow, and flow through a rotating channel. In each example the solution and accompanying analysis of pressure modes rely on rectangular elements, piecewise bilinear basis functions for velocity, and piecewise constant basis functions for pressure, although other element shapes and basis functions could be chosen, just as when λ is held constant in the ordinary penalty method. The findings of this paper are summarized in Section 5.

2. FINITE ELEMENT FORMULATION OF STOKES EQUATIONS

The dimensionless equations of steady, creeping flow are

$$\nabla\cdot\mathbf{T}=\mathbf{0}, \quad \nabla\cdot\mathbf{v}=0, \tag{2a, b}$$

where $\mathbf{T}=-p\mathbf{I}+[\nabla\mathbf{v}+(\nabla\mathbf{v})^{\mathrm{T}}]$ is the stress tensor, $\mathbf{v}$ is velocity (the x and y components in two dimensions are u and v), and p is pressure. When the penalty approach is used, the solenoidal constraint (2b) is replaced by (1).

The Galerkin weighted residual method applied to (2) gives

$$\int_{\Omega}\mathbf{T}\cdot\nabla\phi^{i}\,\mathrm{d}A=\int_{\partial\Omega}\phi^{i}\mathbf{T}\cdot\mathbf{n}\,\mathrm{d}l, \tag{3a}$$

$$\int_{\Omega}\psi^{j}(\nabla\cdot\mathbf{v}+p/\lambda)\,\mathrm{d}A=0, \tag{3b}$$

where ϕ^{i} is an appropriate velocity basis function, ψ^{j} is an appropriate pressure basis function, and $\mathbf{n}$ is the outward pointing unit normal at boundary $\partial\Omega$ of domain Ω. Velocity components and pressure are each approximated by a summation of finite element basis functions:

$$\begin{aligned} u &\simeq u_{\mathrm{d}}\equiv\sum_{i=1}^{n}u_{i}\phi^{i}(x,y),\\ v &\simeq v_{\mathrm{d}}\equiv\sum_{i=1}^{n}v_{i}\phi^{i}(x,y),\\ p &\simeq p_{\mathrm{d}}\equiv\sum_{j=1}^{m}p_{j}\psi^{j}(x,y), \end{aligned} \tag{4}$$

where u_i, v_i and p_j are unknown coefficients of basis functions for velocity components and pressure. We choose for the n ϕ^{i}s bilinear Lagrange basis functions, and for the m ψ^{j}s piecewise constant basis functions. Malkus and Hughes[1] define and discuss the compatibility of this basis set.

Inserting (4) in (3) produces a matrix problem:

$$\begin{aligned} &\mathbf{KV}+\mathbf{Cp}=\mathbf{f} \qquad (5a)\\ &\mathbf{C}^{\mathrm{T}}\mathbf{V}-\mathbf{M}_{\lambda}\mathbf{p}=\mathbf{g} \qquad (5b) \end{aligned} \quad \text{or} \quad \begin{bmatrix}\mathbf{K} & \mathbf{C}\\ \mathbf{C}^{\mathrm{T}} & -\mathbf{M}_{\lambda}\end{bmatrix}\begin{bmatrix}\mathbf{V}\\ \mathbf{p}\end{bmatrix}=\begin{bmatrix}\mathbf{f}\\ \mathbf{g}\end{bmatrix}.$$

The column matrix $\mathbf{f}$ contains boundary conditions on velocity or surface traction, whereas $\mathbf{g}$ contains conditions on velocity alone. $\mathbf{V}$ and $\mathbf{p}$ are column matrices of unknown coefficients u_i and v_i, and p_j. Matrices $\mathbf{K}$ and $\mathbf{C}$ are identical to those defined by Sani *et al.*[10] $\mathbf{K}$ is positive-definite and symmetric for certain choices of boundary conditions and approximates the negative Laplacian operator. $\mathbf{KV}$ represents viscous stress. $\mathbf{C}$ is rectangular and approximates the gradient operator, whereas $-\mathbf{C}^{\mathrm{T}}$, interestingly, approximates the divergence operator. $-\mathbf{C}^{\mathrm{T}}\mathbf{V}$ represents velocity

divergence. The matrix

$$M_{\lambda ij} \equiv \int_{\Omega} \psi^i \psi^j / \lambda \, \mathrm{d}A = \int_{\Omega_i} 1/\lambda \, \mathrm{d}A, \quad \text{if } i = j. \tag{6}$$

is a diagonal matrix for piecewise constant ψs. A discontinuous linear set of ψs would, for example, give rise to a block diagonal $\mathbf{M}_\lambda$.

Because $\mathbf{M}_\lambda$ is diagonal, it can be easily inverted to give pressure as a function of velocity:

$$\mathbf{p} = \mathbf{M}_\lambda^{-1}(\mathbf{C}^{\mathrm{T}}\mathbf{V} - \mathbf{g}). \tag{7}$$

With this the pressure unknowns p_i can be eliminated from (5a) to arrive at

$$(\mathbf{K} + \mathbf{C}\mathbf{M}_\lambda^{-1}\mathbf{C}^{\mathrm{T}})\mathbf{V} = \mathbf{C}\mathbf{M}_\lambda^{-1}\mathbf{g} + \mathbf{f}, \tag{8}$$

a matrix equation for the column matrix $\mathbf{V}$ of the velocity unknowns. Thus (8) can be solved for velocity alone and then pressure can be calculated from (7). Sequential as opposed to simultaneous solution of (7) and (8) is the benefit of the penalty method. It has been shown that with certain boundary conditions the solution $\mathbf{V}$ and $\mathbf{p}$ of (7) and (8), as λ increases uniformly, approaches the solution $\mathbf{V}_{\mathrm{I}}$ and $\mathbf{p}_{\mathrm{I}}$ of the direct mixed interpolation problem:[3,10,11]

$$\mathbf{K}\mathbf{V}_{\mathrm{I}} + \mathbf{C}\mathbf{p}_{\mathrm{I}} = \mathbf{f}, \quad \mathbf{C}^{\mathrm{T}}\mathbf{V}_{\mathrm{I}} = \mathbf{g}. \tag{9}$$

The matrix $\mathbf{C}\mathbf{M}_\lambda^{-1}\mathbf{C}^{\mathrm{T}}$ and vector $\mathbf{C}\mathbf{M}_\lambda^{-1}\mathbf{g}$ for our basis choice are simply and exactly formed by reduced/selective integration as proved by Malkus and Hughes.[3] Neither the pressure basis set ψ^i nor the pressure coefficients $\mathbf{p}$ need be explicitly introduced. We have formed the resulting matrix problem (8) and solved it by Gauss elimination on a CDC Cyber 74 computer that has a unit round-off error of 10^{-14}.

3. DECREASING PENALTY ERROR BY VARIATION OF PENALTY PARAMETER

3.1. Strategies for penalty parameter variation

The penalty parameter λ is made a function of position, i.e. of co-ordinates x and y, and it is chosen to be either positive or *negative*. By apt choice of $\lambda(x, y)$ the *penalty error* in a penalty solution, i.e. the difference between the penalty solution $\mathbf{V}$ and the related direct mixed-interpolation solution $\mathbf{V}_{\mathrm{I}}$, can often be reduced, as demonstrated in Section 4, beyond that achieved by the *conventional penalty method* in which λ is chosen to be equal to a positive constant c_λ.

Although λ can be a continuous function of position, there is no advantage in varying λ in ways that do not alter the weighted continuity equation (3b). The most general λ that is appropriate can be represented by a sum of the weighting (basis) functions ψ^j:

$$\lambda = \sum_{j=1}^{m} \lambda_j \psi^j(x, y) \tag{10}$$

where λ_j are m constants in λ to be specified. Our present scheme rests on piecewise constant ψs, although it could be extended to higher-order ψs, such as bilinear ones, so that λ could be effectively varied within an element.

Penalty error has contributions from two sources: compressibility error, which originates from the approximation (1) of the continuity equation (2b), and digital truncation error, which arises during solution of the matrix problem (8). The penalty parameter can be varied in such a way as to reduce error from both sources; strategies for reducing each are discussed in turn.

Reduction of digital truncation error. The magnitude of digital truncation error when a matrix equation is solved for an unknown vector by Gauss elimination is roughly proportional to the condition number of the matrix multiplied by the unit round-off error of the computer.[22] When λ is constant, the condition number of $\mathbf{S} \equiv \mathbf{K} + \mathbf{C}\mathbf{M}_\lambda^{-1}\mathbf{C}^T$, cf. (8), has been shown[14,16,17] to be roughly proportional to the inverse square of the smallest of all element diameters (see above) multiplied by the penalty parameter. This means that when λ is constant, just a single element of small diameter can inflate digital truncation error throughout the solution, as is demonstrated in examples in Section 4. The inflation becomes acute when to resolve thin boundary layers some elements of small diameter must be employed. A cure is to choose λ_i, the value of λ on element i (cf. (10)), so as to make the value of λ_i/d_i^2 (where d_i is the diameter of element i) the same on each element:

$$\lambda_i = c_\lambda \frac{d_i^2}{\langle d \rangle^2}. \tag{11}$$

The penalty parameter λ_i is set inversely proportional to the square of the element diameter number-averaged over all elements, $\langle d \rangle$, to make fair the comparison between penalty solutions when λ is given by (11) and, for instance, when $\lambda = c_\lambda$. Numerical test cases, however, indicate that λ-variation (11) increases compressibility error.

Reduction of compressibility error. Compressibility error is roughly proportional to λ^{-1} in conventional (namely $\lambda = +c_\lambda$) penalty solutions.[12] The net compressibility, i.e. the creation or annihilation of fluid, averaged on each element is

$$\frac{\int_{\text{element } i} \nabla \cdot \mathbf{v}_d \, dA}{\int_{\text{element } i} dA} = \frac{-\int_{\text{element } i} \frac{p_d}{\lambda} dA}{\int_{\text{element } i} dA} = -\frac{p_i}{\lambda_i}. \tag{12}$$

When the sign of the penalty parameter in the conventional penalty method ($\lambda = +c_\lambda$) is reversed to give the *negative penalty method*, in which $\lambda = -c_\lambda$, digital truncation error and compressibility error are found not to change perceptibly in magnitude, but compressibility error is found to change in sign (see Section 4). If by changing the sign of the penalty parameter from element to element the compressibility error contributed by each element can be made roughly to cancel, the compressibility error can be reduced.

The magnitude of the net compressibility on *one* element defined at (12), cannot be decreased without increasing the magnitude of λ on that element (i.e. λ_i), and thus increasing the likelihood of digital truncation error, as discussed above. The net compressibility of groups or patches of elements, however, can usually be decreased by varying the sign of λ from element to element; the argument is given below. If the net compressibility on most patches of two or more elements were reduced it seems probable that the solution $\mathbf{v}_d$ would improve; this is confirmed by numerical test cases in Section 4. The rationale for variation of penalty parameter to reduce compressibility error follows.

The way to reduce compressibility error is to design λ so that the net compressibility error on each patch of two or more adjacent elements is lowered. One prescription of λ that does this is

$$\lambda_i = \pm c_\lambda a_i / \langle a \rangle, \tag{13}$$

where λ changes sign from element to element in a chequerboard manner. The area of element i is a_i. The number average of all element areas is $\langle a \rangle$, and λ is normalized by it to permit fair comparison with other choices of λ. We call the penalty method in which λ varies according to (13) the *variable penalty method.*

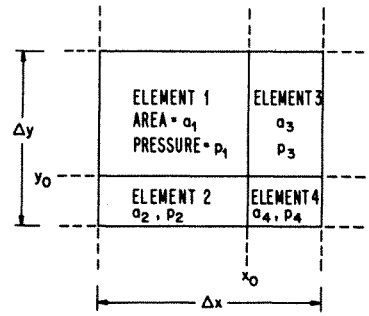

Figure 1. A four-patch of elements

The net compressibility on a patch of elements is

$$\int_{\text{patch}} \nabla\cdot\mathbf{v}_d \, dA = -\int_{\text{patch}} \frac{p_d}{\lambda} dA = -\int_{\text{patch}} \frac{p}{\lambda} dA - \int_{\text{patch}} \frac{(p_d - p)}{\lambda} dA. \tag{14}$$

Pressure p is that which satisfies the Stokes equation (2). If the discrete pressure solution p_d is accurate, the overall error, $p - p_d$ must be small compared to pressure p; for this reason the last integral term in (14) is neglected.

On a patch of two or more adjacent elements the net compressibility with (13) usually is less than with, for instance, $\lambda = +c_\lambda$. This is demonstrated on the patch of four elements shown in Figure 1, although any number of elements could have been chosen.

The net compressibility averaged over a patch of four elements in a conventional ($\lambda = +c_\lambda$) penalty solution is found by expanding p in a Taylor series about x_0 and y_0 (see Figure 1) to be

$$\frac{\int_{4\text{-patch}} \nabla\cdot\mathbf{v}_d \, dA}{\int_{4\text{-patch}} dA} = \frac{-\int_{4\text{-patch}} \frac{p}{c_\lambda} dA}{\int_{4\text{-patch}} dA} = \frac{1}{c_\lambda}[-p|_{x_0,y_0} + O(\Delta x + \Delta y)]. \tag{15}$$

The net compressibility of a *variable* penalty solution, namely (13), averaged over a patch of four elements is found to be

$$\frac{\int_{4\text{-patch}} \nabla\cdot\mathbf{v}_d \, dA}{\int_{4\text{-patch}} dA} = \frac{1}{c_\lambda}\left[\frac{\langle a\rangle}{4}\frac{d^2p}{dxdy} + O(\Delta x + \Delta y)^3\right] \tag{16}$$

by again expanding p in a Taylor series about x_0 and y_0. The penalty parameter variation (13) was designed so that those terms in the Taylor series expansion employed in estimate (16) which are of lower order than $O(\langle a\rangle/c_\lambda)$ cancel; (13) is the only choice of λ which does this. Furthermore, the net compressibility of a variable penalty solution averaged over any patch of two elements is, by the same reasoning as used to derive (16), of $O(\Delta x)$ or $O(\Delta y)$, depending on whether the two elements are in a row or column of the tessellation into rectangular elements; again (13) is the only choice of λ which can achieve this result.

Error estimates for the variable penalty method are derived in two related papers;[21,23] results are summarized here. Under certain restrictions the compressibility error in variable penalty solutions for a discretization into square elements in which all sides are of length h has been proved[21,23] to be of $O[h/c_\lambda]$; whereas that in conventional penalty solutions has been proved[12,13]

to be of $O(1/c_\lambda)$. In the asymptotic limit, as the penalty constant c_λ increases without bound, the compressibility error in both methods approaches zero. However, in the asymptotic limit as element size h approaches zero while c_λ remains constant, compressibility error in variable penalty solutions does approach zero, whereas that of conventional penalty solutions remains finite. In practice both element size h and penalty constant c_λ must be chosen to be finite. Although error estimates[12,13,21,23] give the order of compressibility error, numerical test cases are needed to measure the accuracy of each method when it is applied to non-ideal problems; tests are reported in Section 4.

Not only should the variable penalty method reduce compressibility error, but it is also expected to reduce digital truncation error caused by elements differing drastically in area. This expectation arises because the area-weighting of λ given by (13) can reduce the condition number of $\mathbf{S}$, although not to the extent that can be achieved by making λ proportional to the square of element diameter, as is done in (11).

In preliminary tests, the compressibility error in a penalty solution when λ was chosen by (11) was found to be greater than when λ was proportional to the square of element diameters, as is that in (11), *and* it was also of different signs on adjacent elements. When this latter choice of λ,

$$\lambda_i = \pm c_\lambda \frac{d_i^2}{\langle d \rangle^2}, \tag{17}$$

is employed the method is called the *diameter-weighted, variable penalty method.* Test cases reported in Section 4 indicate that penalty error is less with the variable penalty method than with either the conventional penalty method or the diameter-weighted, variable penalty method.

3.2 Pressure modes in variable penalty solutions

When the variable penalty method is applied to creeping flow under certain boundary conditions, the set of algebraic equations to which it leads can have a solution p_d which differs from the exact solution p by an amount as large as c_λ. When pressure error is so large that it makes the pressure solution p_d of large magnitude (of order c_λ), it also spoils the accuracy of the velocity solution $\mathbf{v}_d$ because compressibility error is proportional to pressure, as (15) and (16) make plain. When the boundary conditions dictated by the physical situation result in large pressure error, they can be avoided by choosing a different set of boundary conditions which is a close approximation to the original set of boundary conditions yet does not result in pressure error of large magnitude.

To predict which boundary conditions result in large pressure error we adapt the theory developed by Sani *et al.*[10,11] For the bilinear velocity and piecewise constant pressure basis set on rectangular elements, they found that when pressure error $p_d - p$ was of large ($O(c_\lambda)$) magnitude it was primarily a combination of two pressure error fields or *modes*: the 'hydrostatic mode' contributes pressure error equal to an amplitude α times

$$\mathbf{p}_h \equiv (1, 1, 1, 1, \ldots)^T, \tag{18}$$

and the 'chequerboard mode' contributes error equal to an amplitude β times

$$\mathbf{p}_c \equiv (+1/a_1, -1/a_2, +1/a_3, \ldots)^T. \tag{19}$$

The area of element i is a_i (see Figure 1).

We now consider several selections of boundary conditions, review the theory of pressure modes for the direct mixed-interpolation and conventional penalty methods, and then extend this theory to the variable penalty method.

Case 1: velocity specified at all boundaries. The matrix

$$\begin{bmatrix} \mathbf{K} & \mathbf{C} \\ \mathbf{C}^{\mathrm{T}} & \mathbf{0} \end{bmatrix} \tag{20}$$

for the direct mixed-interpolation solution of this case has two zero eigenvalues, the eigenfunctions of which are $\mathbf{p}_h$ and $\mathbf{p}_c$. Each of these pressure modes contributes to pressure mode error $\mathbf{p}_m = \alpha\mathbf{p}_h + \beta\mathbf{p}_c$ which satisfies

$$\mathbf{C}\mathbf{p}_m = 0, \tag{21}$$

that is $\mathbf{p}_m$ is orthogonal to the residuals of the discretized momentum equation (9a). To avoid an unsolvable system of algebraic equations, pressure mode error $\mathbf{p}_m$ must also be orthogonal to the residual of the discretized continuity equations: $\mathbf{p}_m^{\mathrm{T}}(\mathbf{C}^{\mathrm{T}}\mathbf{V} - \mathbf{g}) = \mathbf{0}$, which implies $\mathbf{p}_m^{\mathrm{T}}\mathbf{g} = 0$, since $\mathbf{p}_m^{\mathrm{T}}\mathbf{C}^{\mathrm{T}}\mathbf{V} = 0$ (cf. (21)). In most cases $\mathbf{p}_m^{\mathrm{T}}\mathbf{g} = 0$, but there are exceptions described by Sani *et al.*[10,11] where the matrix problem is unsolvable. What follows is restricted to boundary conditions that do satisfy $\mathbf{p}_m^{\mathrm{T}}\mathbf{g} = 0$.

When the conventional penalty method is applied, Sani *et al.*[10,11] found that the pressure mode error $\mathbf{p}_m$ is small. That error is defined here as the difference between pressure solution $\mathbf{p}$ and pressure field $\mathbf{p}_0$:

$$\mathbf{p}_m \equiv \mathbf{p} - \mathbf{p}_0 = \alpha\mathbf{p}_h + \beta\mathbf{p}_c. \tag{22}$$

The pressure field $\mathbf{p}_0$ is chosen to be $\mathbf{M}$-orthogonal to the pressure modes; namely $\mathbf{p}_c^{\mathrm{T}}\mathbf{M}\mathbf{p}_0 = 0$ and $\mathbf{p}_h^{\mathrm{T}}\mathbf{M}\mathbf{p}_0 = 0$. The so-called pressure mass matrix is $M_{ij} \equiv \int_\Omega \psi^i\psi^j \, dA$. When $\lambda = +c_\lambda$, the pressure mass matrix is related to $\mathbf{M}_\lambda$ by

$$\mathbf{M} = c_\lambda \mathbf{M}_\lambda. \tag{23}$$

In terms of $\mathbf{M}$ the Galerkin weighted continuity equation (5b) in the conventional penalty method is

$$\mathbf{M}\mathbf{p} = \mathbf{c}_\lambda(\mathbf{C}^{\mathrm{T}}\mathbf{V} - \mathbf{g}). \tag{24}$$

Taking the inner product of (24) with a pressure mode error $\mathbf{p}_m$ gives $\mathbf{p}_m^{\mathrm{T}}\mathbf{M}\mathbf{p} = c_\lambda \mathbf{p}_m^{\mathrm{T}}(\mathbf{C}^{\mathrm{T}}\mathbf{V} - \mathbf{g}) = 0$. Thus pressure $\mathbf{p}$ is $\mathbf{M}$-orthogonal to both $\mathbf{p}_c$ and $\mathbf{p}_h$. In other words the pressure modes are absent. Pressure $\mathbf{p}$ equals $\mathbf{p}_0$; the pressure solution p_d is a close approximation to the exact pressure p.[10,11]

To extend this analysis to the variable penalty method we make use of

$$\mathbf{A}^n \equiv \begin{bmatrix} a_1^n & 0 & 0 & \cdot & \cdot & \cdot \\ 0 & a_2^n & 0 & \cdot & \cdot & \cdot \\ 0 & 0 & a_3^n & & & \\ \cdot & & & \cdot & & \\ \cdot & & & & \cdot & \\ \cdot & & & & & \cdot \end{bmatrix}, \quad \mathbf{A}^n_{\pm} \equiv \begin{bmatrix} +a_1^n & 0 & 0 & \cdot & \cdot & \cdot \\ 0 & -a_2^n & 0 & \cdot & \cdot & \cdot \\ 0 & 0 & +a_3^n & & & \\ \cdot & & & \cdot & & \cdot \\ \cdot & & & & \cdot & \\ \cdot & & & & & \cdot \end{bmatrix} \tag{25}$$

These matrices conveniently represent the pressure mass matrix, or basis function overlap matrix, $\mathbf{M} = \mathbf{A}^1$, and M_λ in the variable penalty method, $\mathbf{M}_\lambda = \mathbf{A}^0_{\pm}/c_\lambda$. From (18, 19, 25) the pressure modes $\mathbf{p}_c$ and $\mathbf{p}_h$ are related by

$$\mathbf{M}\mathbf{p}_c = \mathbf{A}^1\mathbf{p}_c = \mathbf{A}^0_{\pm}\mathbf{p}_h. \tag{26}$$

The weighted residuals of the momentum equations are still orthogonal to $\mathbf{p}_h$ and $\mathbf{p}_c$. The

continuity equation for the variable penalty method is

$$\mathbf{A}^0_{\pm}\mathbf{p} = c_\lambda(\mathbf{C}^T\mathbf{V} - \mathbf{g}). \tag{27}$$

Taking the inner product of (27) with $\mathbf{p}_m$ gives $\mathbf{p}_m^T\mathbf{A}^0_{\pm}\mathbf{p} = c_\lambda\mathbf{p}_m^T(\mathbf{C}^T\mathbf{V} - \mathbf{g}) = 0$. This results in an equation which determines each of the pressure mode amplitudes: $\mathbf{p}^T\mathbf{A}^0_{\pm}\mathbf{p}_h = 0$ and $\mathbf{p}^T\mathbf{A}^0_{\pm}\mathbf{p}_c = 0$. With (26) the first implies that $\mathbf{p}$ is $\mathbf{M}$-orthogonal to $\mathbf{p}_c$ and thus that the amplitude β of the chequerboard pressure mode is zero. With (26) the second states that $\mathbf{p}^T\mathbf{M}\mathbf{A}^{-2}\mathbf{p}_h = 0$. Thus $\mathbf{p}$ is $\mathbf{M}$-orthogonal to $\mathbf{A}^{-2}\mathbf{p}_h$, not to $\mathbf{p}_h$. If all elements have the same area, $\mathbf{p}$ would be $\mathbf{M}$-orthogonal to $\mathbf{p}_h$ and the amplitude α of the hydrostatic pressure would be zero. If, however, elements differ in area, $\alpha = (-\mathbf{p}_0^T\mathbf{M}\mathbf{A}^{-2}\mathbf{p}_h)/(\mathbf{p}_h^T\mathbf{M}\mathbf{A}^{-2}\mathbf{p}_h)$. Plainly the amplitude of the hydrostatic pressure mode is related to the disparity in element areas.

In Case 1 the hydrostatic mode can be present but it is sizable only when elements vary greatly in area; nevertheless its amplitude α is even then much less than and independent of c_λ and so, as shown in Section 4.2, it may not greatly affect velocity solutions.

Case 2: normal stress specified at a portion of the boundary. Setting a normal stress condition somewhere on the boundary such as at a free surface provides a datum for pressure and the contribution of that condition to the gradient matrix $\mathbf{C}$ makes $\mathbf{C}\mathbf{p}_h \neq 0$, i.e. the weighted momentum residuals depend on the amplitude α of the hydrostatic pressure mode.[10] When the direct mixed-interpolation method is used, the amplitude β of the chequerboard pressure mode is still undetermined.[10] When the conventional penalty method is applied, the amplitude β of the chequerboard pressure mode p_c is zero.

In contrast the variable penalty method gives rise to a chequerboard pressure mode of amplitude $\beta = O(c_\lambda)$ as shown below. This large amplitude pressure mode can induce compressibility error in the velocity solution of order unity because compressibility error is roughly proportional to pressure divided by c_λ: cf. (12). The amplitude β is predicted by taking the inner product of (27) with $\mathbf{p}_h$:

$$\mathbf{p}_h^T\mathbf{A}^0_{\pm}\mathbf{p} = c_\lambda\mathbf{p}_h^T(\mathbf{C}^T\mathbf{V} - \mathbf{g}). \tag{28}$$

The right side of (28) is $O(c_\lambda)$ since $\mathbf{C}\mathbf{p}_h$ is not zero; (28) and (26) give

$$\mathbf{p}_c^T\mathbf{M}\mathbf{p} = c_\lambda\mathbf{p}_h^T(\mathbf{C}^T\mathbf{V} - \mathbf{g}). \tag{29}$$

From (29) and (22) follows the magnitude of the chequerboard pressure mode:

$$\beta = c_\lambda[\mathbf{p}_h^T(\mathbf{C}^T\mathbf{V} - \mathbf{g})]/(\mathbf{p}_c^T\mathbf{M}\mathbf{p}_c).$$

To get an accurate solution by the variable penalty method Case 2 must be avoided.

Case 3: tangential stress specified at a portion of the boundary. If the tangential stress is specified at some portion of the boundary, then the contribution of that condition to $\mathbf{C}$ makes $\mathbf{C}\mathbf{p}_c \neq 0$.[10] The amplitude β of the chequerboard pressure mode is determined by the weighted momentum equations. When the direct mixed interpolation method is used, the amplitude α of the hydrostatic pressure mode is still undetermined.[10] When the conventional penalty method is used, the amplitude α of the hydrostatic pressure mode is zero.[10,11]

From (22) and the inner product of (27) with $\mathbf{p}_c$ the amplitude α of the hydrostatic pressure mode in a variable penalty solution is

$$\alpha = c_\lambda\left[\frac{\mathbf{p}_h^T(\mathbf{C}^T\mathbf{V} - \mathbf{g})}{\mathbf{p}_h^T\mathbf{M}\mathbf{A}^{-2}\mathbf{p}_h}\right] - \left[\frac{\mathbf{p}_h^T\mathbf{M}\mathbf{A}^{-2}(\mathbf{p}_0 + \beta\mathbf{p}_c)}{\mathbf{p}_h^T\mathbf{M}\mathbf{A}^{-2}\mathbf{p}_h}\right].$$

This hydrostatic pressure mode of $O(c_\lambda)$ forces a penalty error of $O(1)$ in velocity, as the chequerboard pressure mode does in Case 2.

Case 4: tangential and normal stress specified at a portion of the boundary. If a tangential stress condition and a normal stress condition are each specified at the same or different portions of the boundary, the amplitudes α and β of the pressure modes are determined by the weighted momentum equations through the contribution of the boundary conditions to the gradient matrix $\mathbf{C}$.[10,11] The amplitude of pressure is ordinarily not large.[10,11]

To summarize, either velocities must be specified at all boundaries (Case 1) or both tangential and normal stress conditions must be imposed on some portion of the boundary to avoid penalty error induced by sizable pressure mode error. Other choices (Cases 2 and 3) of boundary conditions must be avoided for they can produce large ($O(c_\lambda)$) pressure modes which result in penalty error in velocity of order unity.

4. CASE STUDIES

Three flow situations are solved here by both the variable (λ given by (13)) and the conventional ($\lambda = +c_\lambda$) penalty methods. The negative ($\lambda = -c_\lambda$) and the diameter-weighted variable penalty methods are each compared to the variable and conventional penalty methods in one case. All three test cases are solved on a square domain tessellated into 100 (ten by ten) rectangular elements. Velocity is approximated by a bilinear basis set. The comparisons reveal that in the cases tested the variable penalty method is never less accurate than the others unless pressure modes intrude.

4.1 *Planar Poiseuille flow*

Pressure-driven flow between parallel solid planes is analysed by penalty finite element methods. Two different sets of boundary conditions are imposed. One allows a chequerboard pressure mode, the other gives a close approximation to the exact velocity field.

Example: whole channel. Figure 2 shows the domain tessellation into square elements of equal size and the boundary conditions imposed. Velocity is specified at the inflow boundary and at the solid walls as an essential boundary condition. At the outflow boundary, normal stress is specified

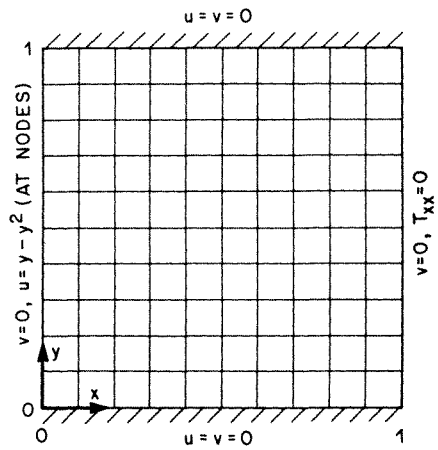

Figure 2. Whole channel, plane Poiseuille flow problem

as a natural boundary condition. No shear stress condition is specified there; instead, the velocity tangential to the boundary, v, is set to zero there as an essential boundary condition.

Were the direct mixed-interpolation method used, the result would be the exact solution, i.e. $v = 0$ and $u = y - y^2$, at all nodes. When conventional penalty solutions are calculated with different choices of penalty constant c_λ, those solutions agree with the mixed-interpolation solution within an error of $O(1/c_\lambda)$ until c_λ becomes large enough that digital truncation error becomes appreciable. When the variable penalty method is applied, a chequerboard pressure mode with an amplitude of $O(c_\lambda)$ arises and causes such inaccuracy in both the pressure and velocity that solutions are not meaningful. The boundary conditions in this example are those in Case 2 of Section 3.2, in which the chequerboard pressure mode is predicted to arise.

This pressure mode can be avoided by specifying a shear stress condition somewhere on the boundary. A shear stress distribution could be specified at the outflow boundary, or a shear-free condition could be specified along the symmetry plane as is done in the next example.

Example: half channel. Figure 3 shows that same tessellation and boundary conditions as

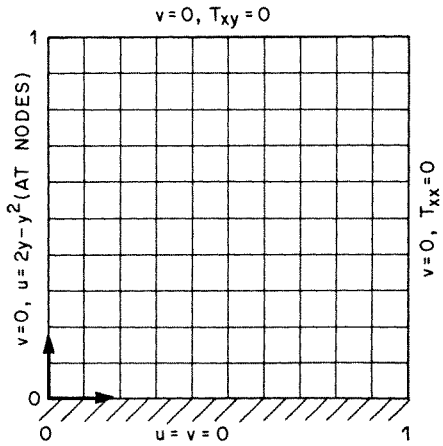

Figure 3. Half channel, plane Poiseuille flow problem. (Based on Figure 2 from *Lectures in Applied Mathematics*, (1985), 'Improved flux calculations for viscous incompressible flow by the variable penalty method', H. Kheshgi and L. E. Scriven, Volume 22, by permission of the American Mathematical Society.)

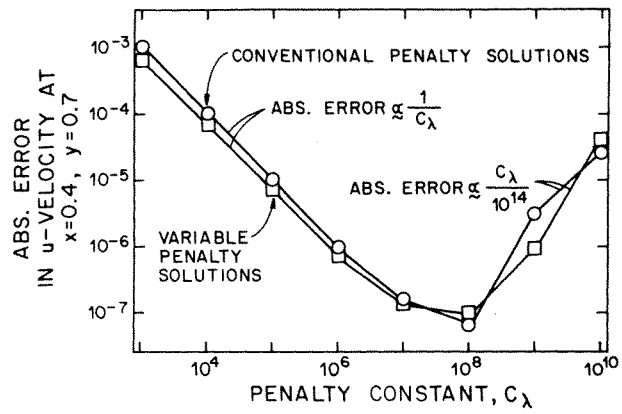

Figure 4. Absolute error, $v_d - v$, in variable and conventional penalty solutions at a characteristic node: half channel, plane Poiseuille flow problem

imposed above except for the symmetry condition at $y = 1$ and, accordingly, a different inflow velocity profile. Because both shear and normal stress conditions are imposed (as natural conditions), pressure modes are too small in amplitude to perceive, as predicted in Case 4 of Section 3.2. Again, the direct mixed-interpolation solution is identical to the exact solution, $v = 0$ and $u = 2y - y^2$, at all element nodes.

The absolute value of error (deviation from the exact solution) in u-velocity at a node located at $x = 0{\cdot}4$ and $y = 0{\cdot}7$ is plotted in Figure 4 against the penalty constants, c_λ, chosen for both conventional penalty solutions and variable penalty solutions. For c_λ less than 10^7 the compressibility error in both methods is nearly proportional to $1/c_\lambda$. The constant of proportionality is slightly smaller in variable penalty solutions, which are thus slightly superior. Variable penalty solutions grow more accurate than do conventional penalty solutions at points further and further downstream. At c_λ greater than 10^8, the penalty error is due to digital truncation and is approximately proportional to c_λ. Both methods incur about the same magnitude of digital truncation error.

In some respects the accuracy is greatly improved by alternating the sign of the penalty parameter. Figure 5 shows the absolute value of the deviation from the corresponding mixed interpolation solution of volumetric flux out of the channel. The compressibility error in the conventional penalty solutions is proportional to $1/c_\lambda$, whereas that in the variable penalty solutions is proportional to $1/c_\lambda^2$, which of course is smaller. This improvement is easily explained. Pressure varies linearly in the channel and does not contribute to the net compressibility over a patch of, for instance, four elements, as shown at (16). The compressibility error in pressure that remains is a higher-order term.[24] Compressibility error does not build up with distance downstream as it does in conventional penalty solutions.

4.2 Lid-driven cavity flow

The solution of flow in a lid-driven cavity by the conventional, negative, diameter-weighted variable and variable penalty methods is calculated when elements are square and of equal area to test the variable penalty method when the pressure field is not linear, and when some elements are small and some skinny to test how much the variable penalty method reduces digital truncation error, compared to other methods.

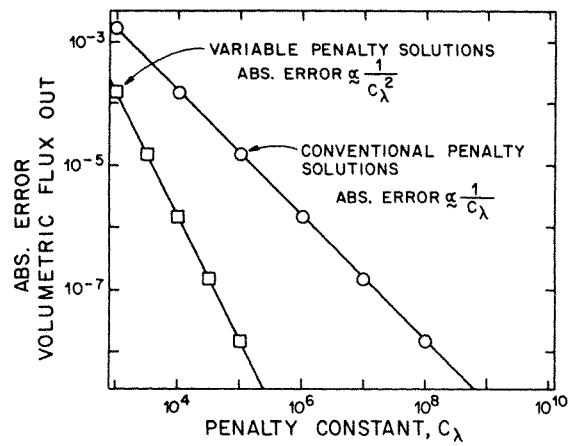

Figure 5. Penalty error in volumetric flux, i.e. the difference between that found by a penalty method and the direct mixed-interpolation method, through the outflow boundary: half channel, plane Poiseuille flow problem. (Based on Figure 3 from *Lectures in Applied Mathematics*, (1985), 'Improved flux calculations for viscous incompressible flow by the variable penalty method', H. Kheshgi and L. E. Scriven, Volume 22, by permission of the American Mathematical Society.)

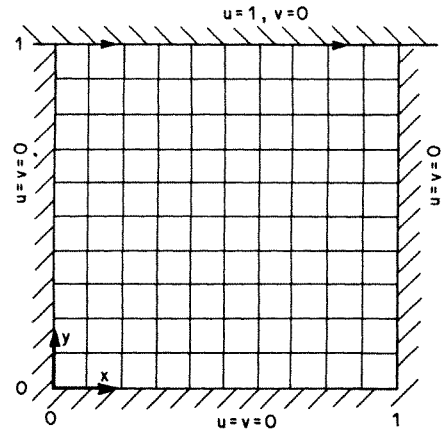

Figure 6. Lid-driven cavity problem with square elements of constant area

Example: square elements. Figure 6 shows the element tessellation and boundary conditions for this problem. As chosen the elements have equal areas and the velocities are specified at all boundaries, as in Case 1 of Section 3.2; no pressure modes are detected in either conventional or variable penalty solutions.

Again, solutions were calculated for a wide range of c_λ. Figure 7 shows the penalty error in u-velocity at a selected point ($x = 0{\cdot}4$, $y = 0{\cdot}8$) in the conventional penalty method ($\lambda = c_\lambda$), the negative penalty method ($\lambda = -c_\lambda$), and the variable penalty method (in this case $\lambda = \pm c_\lambda$). At c_λ greater than 10^8, the error is due to digital truncation and is of nearly the same magnitude in solutions calculated with the three methods. At c_λ less than 10^8, the error is due to compressibility and is proportional to $1/c_\lambda$ in solutions calculated with the three methods. The variable penalty method again has a smaller proportionality constant and is thus more accurate than either the negative or conventional penalty methods. The proportionality constant of the negative penalty solutions is of the same magnitude, yet opposite in sign from that of the conventional penalty solutions. If negative and conventional penalty solutions are added together and divided by two, the $O(1/c_\lambda)$ compressibility errors cancel and the average is accurate to the next higher order, namely $O(1/c_\lambda^2)$, as demonstrated by Figure 8.

In the flow domain there are special points where velocities predicted by variable penalty

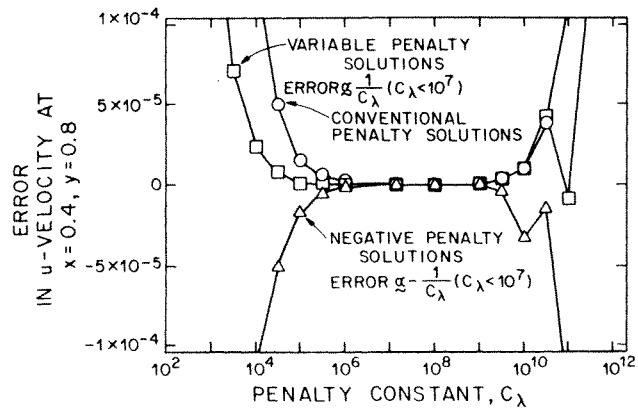

Figure 7. Penalty error, $\mathbf{V} - \mathbf{V}_I$, at a characteristic node: driven cavity problem with square elements

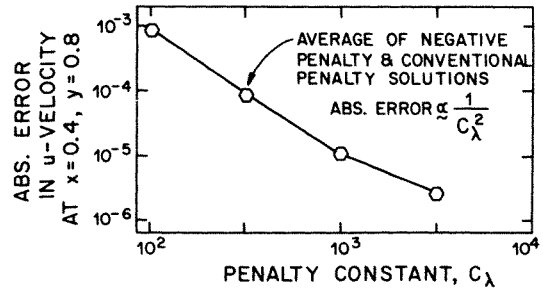

Figure 8. Penalty error, $\mathbf{V} - \mathbf{V}_I$, of the average of conventional and negative penalty solutions: driven cavity problem with square elements

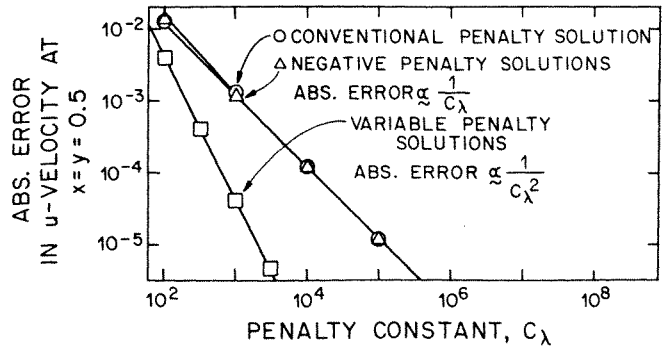

Figure 9. Penalty error, $\mathbf{V} - \mathbf{V}_I$, at a node along the vertical centreline of the cavity: driven cavity problem with square elements

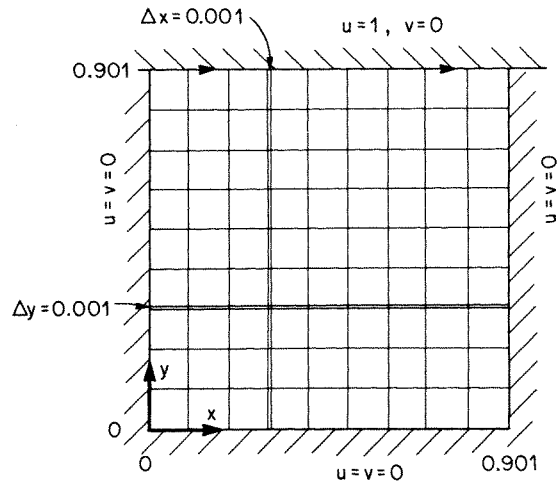

Figure 10. Lid-driven cavity problem with element areas that vary greatly

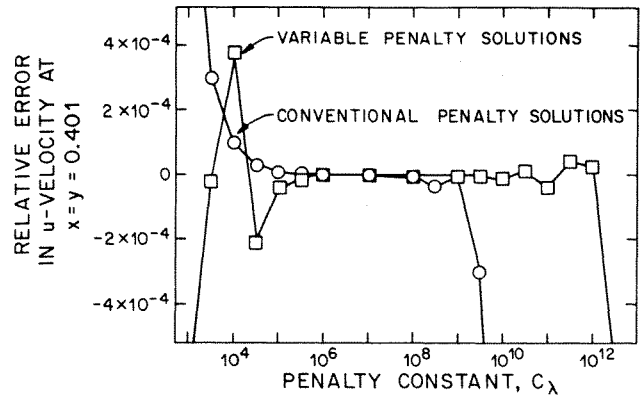

Figure 11. Penalty error, $\mathbf{V} - \mathbf{V}_I$, at a characteristic node: driven cavity problem with unequal element areas

solutions are more accurate than $O(1/c_\lambda)$. Figure 9 shows the penalty error in the u-velocity at the centre node of the domain described in Figure 6 when calculated with the three solution methods. The penalty error in the conventional and negative penalty solutions is of $O(1/c_\lambda)$ over the range of c_λ shown in Figure 9. Penalty error in variable penalty solutions is roughly proportional to $1/c_\lambda^2$.

Example: uneven element areas. To study the effect of varying element size on the accuracy of penalty solutions, the driven-cavity problem shown in Figure 10 is solved. Velocities are specified on all boundaries. According to Case 1 of Section 3.2, pressure modes should have no amplitude in conventional penalty solutions; there should be a hydrostatic pressure of $O(1)$, however, in variable penalty solutions.

In this example, variable penalty solutions contain a hydrostatic pressure of amplitude $\alpha \simeq 10$. This pressure does cause slightly greater compressibility error in variable penalty solutions than in conventional penalty solutions as shown in Figure 11. When elements vary greatly in size the area-weighting of λ given by (13) is expected to reduce significantly the condition number of $\mathbf{S}$ and thus the magnitude of digital truncation error in variable penalty solutions. That this expectation is realized is seen vividly in Figure 11 where variable penalty solutions are accurate although c_λ is nearly a thousand times larger than for conventional penalty solutions.

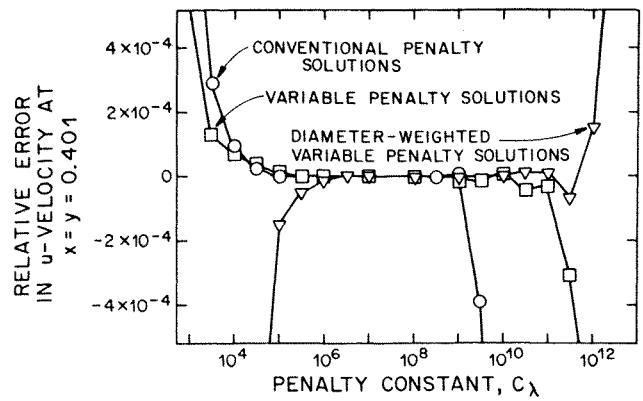

Figure 12. Penalty error, $\mathbf{V} - \mathbf{V}_I$, at a characteristic node: driven cavity problem with unequal element areas and a traction free condition at one node

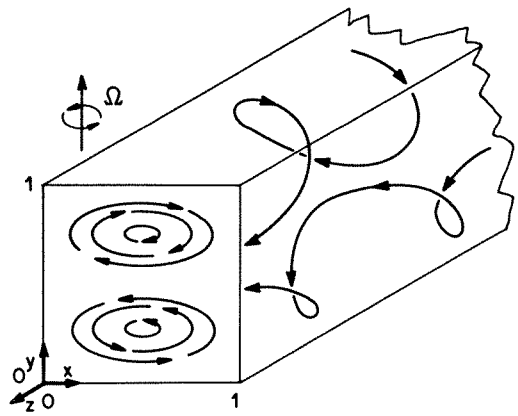

Figure 13. Flow through a rotating square channel. (Based on Figure 4 from *Lectures in Applied Mathematics*, (1985), 'Improved flux calculations for viscous incompressible flow by the variable penalty method', H. Kheshgi and L. E. Scriven, Volume 22, by permission of the American Mathematical Society.)

The hydrostatic pressure can be removed from variable penalty solutions by requiring that traction vanish at one boundary point, in this case $x = 0{\cdot}301$ and $y = 0$; the effect on the solution is imperceptible. Figure 12 shows that when this is done the variable penalty solutions are slightly more accurate than conventional penalty solutions when c_λ is less than 10^7. Furthermore, the variable penalty method is still much more accurate when c_λ is greater than 10^7.

The penalty error in the diameter-weighted variable penalty method (λ given by (17)) is shown in Figure 12. Although it is expected to reduce the global matrix condition number and thus the amount of digital truncation error slightly more than does the variable penalty method, it results in much more compressibility error when c_λ is less than 10^7. It appears not to have any advantage over the variable penalty method and we consider it no further.

4.3 Flow through a rotating channel

Flow through a square channel rotating about an axis perpendicular to the channel top is shown in Figure 13. As Ekman number, the ratio of viscous to Coriolis force, falls boundary layers form along the solid walls and become *narrow*.[26] When the Ekman number is 10^{-6}, the thin Ekman layers present are resolved by choosing elements which vary in dimension from 0·0002 to 0·495

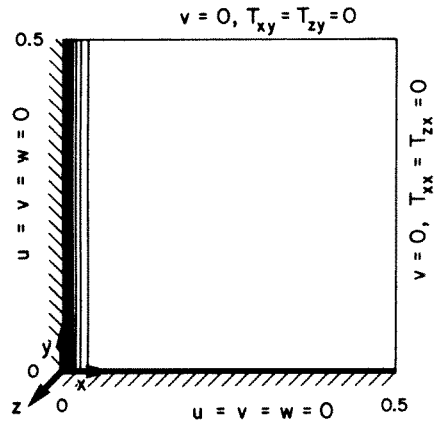

Figure 14. Rotating channel problem with elements designed to resolve thin boundary layers

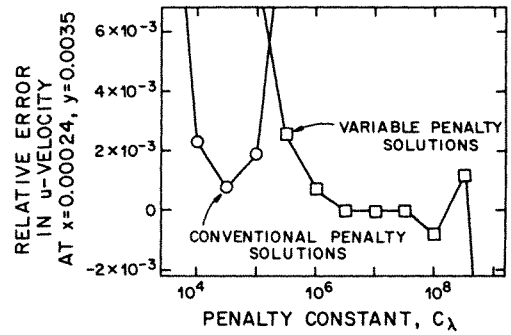

Figure 15. Penalty error, $\mathbf{V} - \mathbf{V}_I$, at the node nearest the corner of a rotating channel

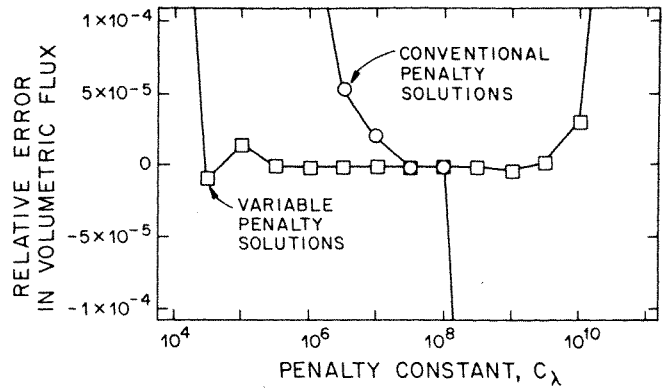

Figure 16. Penalty error in volumetric flux through a rotating channel. (Based on Figure 5 from *Lectures in Applied Mathematics*, (1985), 'Improved flux calculations for viscous incompressible flow by the variable penalty method', H. Kheshgi and L. E. Scriven, Volume 22, by permission of the American Mathematical Society.)

times the channel height. The presumed symmetry of the flow allows this problem to be solved for pressure and the three components of velocity on just a quarter of the two-dimensional channel cross-section. Both normal and shear stress conditions are specified on the boundary, as shown in Figure 14, cf. Case 4 of Section 3.2.

The combination of small Ekman number and greatly varying element size prevents accurate solution by the conventional penalty method. Figure 15 shows the penalty error at that node which is within the channel and closest to the channel corner. At this node the digital truncation error makes conventional penalty solutions inaccurate; the variable penalty solution remains accurate when c_λ is chosen between 10^6 and 10^8.

The volumetric flux through the channel is found by integrating the z-component of velocity across the channel. Figure 16 shows the relative penalty error in volumetric flux in the conventional and variable penalty solutions. The range of c_λ over which the conventional method is accurate is narrow and unreliable. The corresponding range of the variable penalty method is broad.

5. CONCLUSION

Variable penalty parameters are easy to implement and can produce more accurate solutions than are achievable by the conventional penalty method, as is clear from the problems tested. Moreover, the variable penalty method is capable of solving certain problems, e.g. with thin boundary layers,

on short word-length computers; the conventional penalty method cannot. Further application and study of the variable penalty method for the solution of other constrained problems and using higher order basis functions is recommended.

ACKNOWLEDGEMENTS

We thank Professor M. Luskin of the School of Mathematics, University of Minnesota, for insightful advice. This work was supported by the Fluid Mechanics Program of the U.S. National Science Foundation and à grant-in-aid from the Kodak Foundation.

REFERENCES

1. D. S. Malkus and T. J. R. Hughes, 'Mixed finite element methods—reduced and selective integration techniques: a unification of concepts', *Comp. Mech. Appl. Mech. Eng.*, **15,** 63 (1978).
2. C. Taylor and P. M. Hood, 'A numerical solution of the Navier–Stokes equations using FEM techniques,' *Comp. Fluids*, **1,** 73 (1973).
3. O. C. Zienkiewicz, 'Constrained variational principles and penalty function methods in finite element analysis', in G. A. Watson (ed.) *Lecture Notes in Mathematics: Conference on the Numerical Solution of Differential Equations*, Springer-Verlag, Berlin, 1974.
4. J. N. Reddy, 'On penalty function methods in the finite element analysis of flow problems', *Int. j. numer. methods fluids*, **2,** 151–171 (1982).
5. T. J. R. Hughes, W. K. Liu and A. Brooks, 'Finite element analysis of incompressible viscous flow by the penalty function formulation', *J. Comp. Phys.*, **30,** 1 (1979).
6. M. Bercovier and M. S. Engelman, 'A finite element for the numerical solution of viscous incompressible flows', *J. Comp. Phys.*, **30,** 181 (1979).
7. R. Courant, K. Friedrichs and J. Lewy, 'Uber die partieller differenzengleichungen der mathematischen physik', *Mathematische Annalen*, **100,** 32 (1928). English translation: *IBM J.* (1967).
8. M. S. Engelman, R. L. Sani, P. M. Gresho and M. Bercovier, 'Consistent vs. reduced integration penalty methods for incompressible media using several old and new elements', *Int. j. numer. methods fluids*, **2,** 25–42 (1982).
9. J. T. Oden, 'Penalty method and reduced integration for the analysis of fluids', in J. N. Reddy (ed.) *Penalty-Finite Element Methods in Mechanics*, AMD-Vol. 51, ASME, 21–32 (1982).
10. R. L. Sani, P. M. Gresho, R. L. Lee and D. F. Griffiths, 'The cause and cure (?) of the spurious pressures generated by certain FEM solutions of the incompressible Navier–Stokes equations: part I', *Int. j. numer. methods fluids*, **1,** 17–43 (1981).
11. R. L. Sani, P. M. Gresho, R. L. Lee, D. F. Griffiths and M. S. Engelman, 'The cause and cure (?) of the spurious pressures generated by certain FEM solutions of the incompressible Navier–Stokes equations: part II', *Int. j. numer. methods fluids*, **1,** 171–204 (1981).
12. R. Temam, *Navier–Stokes Equations*, North-Holland Press, Amsterdam, 1977.
13. V. Girault and P. A. Raviart, 'Finite element approximations of the Navier–Stokes equations', *Lecture Notes in Math.*, No. 749, Springer-Verlag, 1979.
14. P. Bar-Yoseph, 'A comparison of various finite element schemes for the solution of the Navier–Stokes equations in rotating flow problems', in D. H. Norrie (ed.) *Proc. Third Int. Conf. Finite Elements Flow Problems, Vol. 1*, Banff, Alberta, 1980.
15. H. S. Kheshgi and L. E. Scriven, 'Penalty finite element analysis of unsteady free surface flows', in R. H. Gallagher *et al.* (eds.) *Finite Elements in Fluids, Vol. 5*, Wiley, New York, 1983.
16. I. Fried, 'Bounds on the extremal eigenvalues of the finite element stiffness and mass matrices and their spectral condition number', *J. Sound and Vibration*, **22,** 407 (1972).
17. I. Fried, 'Influence of Poisson's ratio on the condition of the finite element stiffness matrix', *Int. J. Solids Structures*, **9,** 323 (1973).
18. R. S. Marshall, J. C. Heinrich and O. C. Zienkiewicz, 'Natural convection in a square enclosure by a finite-element, penalty function method using primitive fluid variables', *Num. Heat Transfer*, **1,** 315 (1978).
19. C. D. Upson, P. M. Gresho and R. L. Lee, 'Finite element simulations of thermally induced convection in an enclosed cavity', *Lawrence Livermore Laboratory Report UCID-18602*, 1980.
20. H. S. Kheshgi and L. E. Scriven, 'Penalty finite element analysis of time-dependent two-dimensional free surface film flows', in T. Kawai (ed.) *Finite Element Flow Analysis*, University of Tokyo Press, Tokyo, 1982.
21. H. S. Kheshgi and M. Luskin, 'On the variable sign penalty method for the computation of solutions to the Navier–Stokes equation', in J. A. Smoller (ed.) *Contemporary Mathematics, Vol. 17*, Amer. Math. Soc., Providence, Rhode Island, 1983.
22. E. Isaacson and H. B. Keller, *Analysis of Numerical Methods*, Wiley, New York, 1966.

23. H. S. Kheshgi and M. Luskin, 'Analysis of the finite element variable penalty method for Stokes equations', *Math. Comp.* (in press 1985).
24. H. S. Kheshgi and M. Luskin, 'Improved flux calculations by the variable penalty method', *Lectures in Applied Mathematics, Vol. 22*, American Mathematical Society, 1984.
25. R. S. Falk, 'An analysis of the penalty method and extrapolation for the stationary Stokes equations', R. Vichnevetsky (ed.) *Advances in Computer Methods for Partial Differential Equations*, 1975.
26. H. S. Kheshgi and L. E. Scriven, 'Viscous flow through a rotating square channel', *Phys. Fluids* (in press 1985).